

Neutron emission from the photon-induced reactions in ultraperipheral ultrarelativistic heavy-ion collisions

P. Jucha,^{1,*} M. Klusek-Gawenda,^{1,†} A. Szczurek,^{1,2,‡} M. Ciemala,^{1,§} and K. Mazurek^{1,¶}

¹*Institute of Nuclear Physics PAN, ul. Radzikowskiego 152, PL-31342 Kraków, Poland*

²*College of Natural Sciences, Institute of Physics,
University of Rzeszów, ul. Pigonía 1, PL-35-310 Rzeszów, Poland*

(Dated: March 20, 2025)

The ultraperipheral collisions are the source of various interesting phenomena based on photon-induced reactions. We calculate cross sections for single and any number of n, p, α , γ -rays in ultraperipheral heavy-ion collision for LHC energies.

We analyze the production of a given number of neutrons relevant for a recent ALICE experiment, for $\sqrt{s_{NN}} = 5.02$ TeV. In our approach, we include both single and multiple photon exchanges as well as the fact that not all photon energies are used in the process of equilibration of the residual nucleus. We propose a simple two-component model in which only part of photon energy E_γ is changed into the excitation energy of the nucleus ($E_{exc} \neq E_\gamma$) and compare its results with outcomes of HIPSE and EMPIRE codes. The role of high photon energies for small neutron multiplicities is discussed. Emission of a small number of neutrons at high photon energies seems to be crucial to understand the new ALICE data. All effects work in the desired direction, but the description of the cross section of four- and five-neutron emission cross sections from first principles is rather demanding. The estimated emission of charged particles such as protons, deuterons and α is shortly discussed and confronted with very recent ALICE data, obtained with the proton Zero Degree Calorimeter.

I. INTRODUCTION

The photon-induced reactions are a wonderful playground for investigation of various phenomena, starting from Giant Dipole Resonance (GDR) by particle emission from excited nuclei and even fission of the excited nucleus up to the production of high-energy particles such as Deltas and other nucleon resonances.

The collision of the two lead nuclei with ultrarelativistic velocities are the subject of investigation of many groups associated with RHIC [1] and the LHC [2, 3]. Depending on the impact parameters, for central collision, the quark-gluon plasma physics is crucial, but for ultraperipheral collisions (UPC), other, more nuclear physics type effects start to play the dominant role.

The exchange of the photon between colliding nuclei leads to electromagnetic disintegration of the nuclei. The Coulomb dissociation is an important ingredient influencing the lifetime of nuclear beams at RHIC and the LHC [4].

The main physics idea behind the appearance of such processes is quite simple: the motion of charged nuclei is the source of moving electromagnetic (EM) fields. The quasi-real photons created by the EM field of one nucleus, can hit the second nucleus and excite it. The standard Coulomb interaction of two charged nuclei with $Z_1 = Z_2 = 82$ predicts the distribution of the excitation energy of

such spectators up to about 50 MeV. Thus, our previous calculations presented in Ref. [5] have been restricted to this value. However, the new measurements of the ALICE collaboration [2] suggest that there are other phenomena which should be taken into consideration when the nucleus excitation energy achieves higher values. In the present study, we discuss a range of a photon energy relevant for production of a few neutrons.

In the UPC the excitation of a nucleus is obtained naively with a convolution of the photon flux and the photoabsorption cross section. Detailed calculations requires precise modeling of the energy transfer to the nucleus and estimation of the neutron emission from the nucleus, both in preequilibrium and equilibrium stage. The cross section for neutron emission can be also obtained by similar convolution of the photon flux with the photoneutron cross section. The latter was measured up to 140 MeV photon energies [6].

It is very difficult to measure precisely neutrons for large photon energies in $\gamma + A$ collisions. However, it is easier to detect neutrons in UPC of heavy ions due to the narrow emission cone. The ALICE experiment provides neutron multiplicities, but other particles, such as protons and alpha particles, were not measured and discussed so far.

In Ref. [5] we assumed that the full photon energy is transformed into excitation energy of the nucleus ($E_{exc} = E_\gamma$) and the GEMINI++ program [7] was used to deexcite the hot nucleus, assuming Hauser-Feshbach [8] particle cascade model. Furthermore we compared our results with the production of multiple neutrons (up to 3 neutrons) as measured by the ALICE collaboration in UPC for $\sqrt{s_{NN}} = 2.76$ TeV, see Ref. [9]. A new valuable result was obtained recently by the ALICE collaboration for $\sqrt{s_{NN}} = 5.02$ TeV [2], where up to 5 neutrons were

*Electronic address: Pawel.Jucha@ifj.edu.pl

†Electronic address: Mariola.Klusek-Gawenda@ifj.edu.pl

‡Electronic address: Antoni.Szczurek@ifj.edu.pl

§Electronic address: Michal.Ciemala@ifj.edu.pl

¶Electronic address: Katarzyna.Mazurek@ifj.edu.pl

measured. As it will be discussed below, our old approach leads to a smaller number of neutron emissions than measured by the ALICE collaboration.

In this paper we shall discuss how the new ALICE result is related to the underlying physics. The presented method consists of three stages:

- (1) the calculation of the photon flux within the equivalent photon approximation (EPA);
- (2) absorption of photons by nucleus and excitation energy estimation using: a simple two-component model (TCM), Heavy Ion Phase – Space Exploration (HIPSE) [10] or Nuclear Reaction Model Code System for Data Evaluation (EMPIRE) [11];
- (3) deexcitation of the hot nucleus in GEMINI++ statistical code.

Then the results are compared with experimental data. The novelty is a proposition of a simple two-component model (TCM) where $E_{exc} < E_\gamma$, consistent with $\gamma + A \rightarrow A' + kn$ experimental data for $E_\gamma < 140$ MeV. The role of high-energy photon scattering off nuclei will be emphasized.

II. THEORETICAL METHODS

A. Photon flux

The moving charged nuclei generate the photon flux, which is calculated using the equivalent photon approximation (EPA) [12]. Analytic formula for point-like nucleus can be found e.g. in [13]:

$$N(\omega, b) = \frac{\alpha Z^2}{\pi^2} \frac{u^2}{\beta^2 \omega b^2} \left(K_1^2(u) + \frac{1}{\gamma_{LAB}^2} K_0^2(u) \right). \quad (1)$$

For extended charge, one has:

$$N(\omega, b) = \frac{Z^2 \alpha_{em}}{\pi^2 \beta^2} \frac{1}{\omega b^2} \times \left| \int d\chi \chi^2 \frac{F(\frac{\chi^2 + u^2}{b^2})}{\chi^2 + u^2} J_1(\chi) \right|^2. \quad (2)$$

Above ω is photon energy and b is transverse distance of photons from the emitting nucleus. If we are interested in photon energy in the rest frame of the absorbing nucleus: $\omega = E_\gamma$. The electromagnetic form factor of the nucleus $F(\frac{\chi^2 + u^2}{b^2})$ depends on $u = \frac{\omega b}{\gamma_{CM} \beta}$, $\gamma_{CM} = \frac{1 + \beta^2}{1 - \beta^2}$, χ is an auxiliary dimensionless variable related to photon transverse momentum via the relation $\chi = k_\perp b$. In realistic case $F(\frac{\chi^2 + u^2}{b^2})$ is calculated as a Fourier transform of the nucleus charge density.

The EPA method allows us to calculate the impact parameter space distribution of photons produced by fast moving charged sources. In the Eq. (2), $N(\omega, b)$ means rather $\frac{dN(\omega, b)}{d\omega d^2b}$ but is used to shorten other more complicated formulas. The photon flux distribution for ultra-peripheral collisions of ^{208}Pb nuclei with the energy $\sqrt{s_{NN}}$

= 5.02 TeV are shown in Fig. 1. Photons are produced typically with energies below 20 MeV, but there is still a sizable probability to generate highly energetic γ -rays. This energetic quasi-real photons could appear for the impact parameter $b = R_{A_1} + R_{A_2} > 14$ fm, where UPC is considered. The nucleus absorbs such photons, raising its internal energy, and follows typical nuclear processes such as γ -rays emission and particle evaporation, fission, or even multifragmentation.

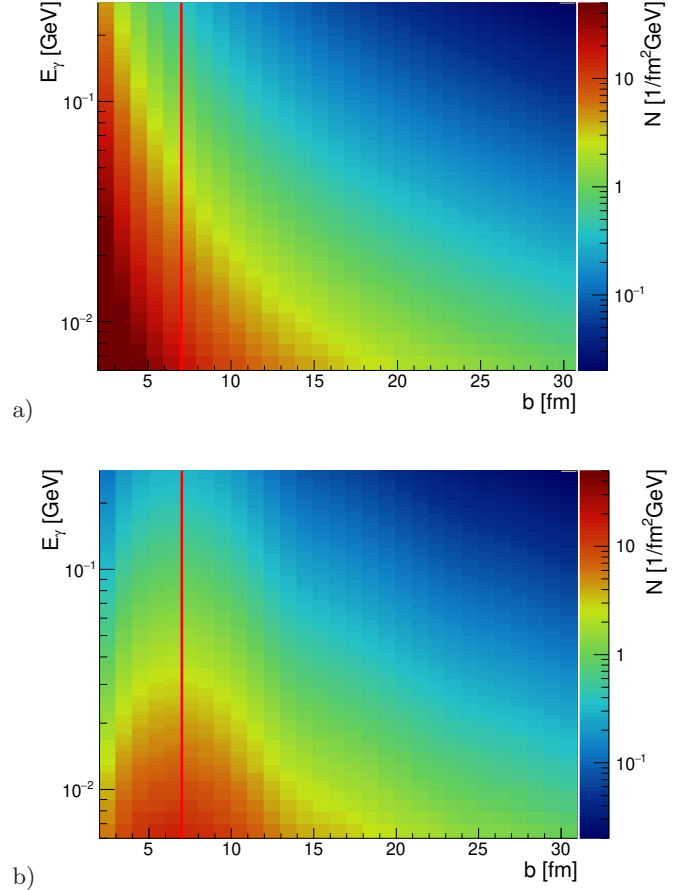


FIG. 1: Calculated photon flux dependence on photon energy and impact parameter. The $b_1 = R_A$ impact parameter is marked explicitly by the red line. a) Analytic formula (Eq. (1)); b) Flux obtained with realistic form factor (Eq. (2)). Here, the Fermi functional form of charge density was used to calculate the form factor.

The flux of photons depends on the transverse distance from the emitting nucleus, where quasi-real photons are emitted. This is illustrated in Fig. 2. In our calculations, one has to integrate over all configurations of the impact parameter space when quasi-real photon associated with one nucleus hits the second nucleus. The impact parameter $b_1 = R_A$ configuration is a limiting configuration which leads to the excitation of the second nucleus. In the present calculations, the impact parameter b_1 is integrated in the range 7 – 10⁹ fm.

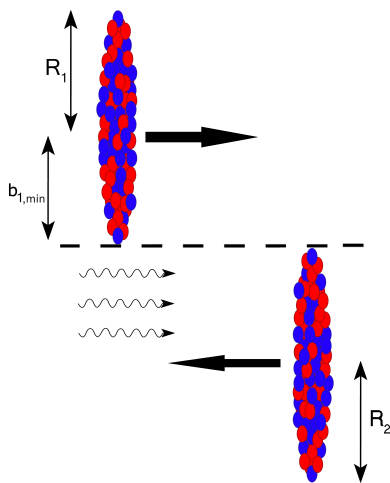


FIG. 2: The impact parameter range of quasi-real photons emitted by one nucleus which excite the second nucleus.

B. Existing generators for photon nucleus interaction

A first dedicated $\gamma + A$ generator was presented in Ref. [14]. This generator was valid up to $E_\gamma = 1$ GeV. The RELDIS code [15] seems to be currently the best photon-induced intranuclear cascade code, at least up to a few GeV photon energy as it takes into account a multitude of hadronic final states as well as corresponding secondary interactions¹. There the integration is done over the transverse distance between colliding nuclei.

In Ref. [16] many multi-body channels were discussed and Monte Carlo calculations confronted with existing experimental data for a few body final states. For multipion final states ($3\pi - 8\pi$) an approximate statistical approaches were considered and discussed. The consequences for subsequent neutron emission in the process of residual nucleus deexcitation were not discussed in [16]. The results of the study in [16] were implemented into the RELDIS code. We do not know about any detailed experimental study of neutron emission induced by high-energy photons.

At higher photon energies ($E_\gamma > 2 - 5$ GeV) the physics again changes and photon interaction directly with partons in protons and neutrons must be included.

The intranuclear model in [17] tried to describe neutron, proton and pion emission at energies below the two-pion production threshold. The Monte Carlo generator based on the dual parton model (DPMJET-III) [18, 19] is capable of simulating hadron-hadron, hadron-nucleus, nucleus-nucleus, photon-hadron, photon-photon and photon-nucleus interactions from a few GeV up to the highest cosmic ray energies.

The STARlight generator [20], often used for ultraperipheral collisions, can compute cross sections and generate events for two-photon and photonuclear interactions accompanied by mutual Coulomb excitation. These processes involve three or four photons: one or two for the photonuclear or two-photon interaction, plus one to excite each nucleus. The program can also calculate cross sections for reactions involving mutual excitation to a Giant Dipole Resonance, which typically decays through the emission of a single neutron. STARlight gives only fractions of the $0n0n$, $1n1n$, $Xn0n$, and $XnXn$ categories. In [21], a very useful UPC Monte Carlo code **n⁰0n** is described which parametrizes rather existing experimental data for $\gamma + A \rightarrow A' + kn$.

Neutron production from excited nuclear system will be discussed in future also at the EIC. A BeAGLE Monte Carlo generator has already been constructed. It allows to calculate average neutron multiplicity in $e + A$ collisions [22]. BeAGLE uses intranuclear cascade DPMJet and PYTHIA-6 for hadronization. The geometry in BeAGLE is, however, somewhat different (virtual photons) than the geometry needed in UPC (quasi-real photons).

A color dipole model would be the best starting point in this region of energy. However, a future approach would require the calculation of the energy transfer to the nucleus due to the interaction of the color dipole with the nuclear matter and modeling of the subsequent neutron emissions. Again a very challenging task. Only emission of dijet and pions was considered [23] within the dual photon approach.

C. Towards simple dynamical model

Now, we wish to consider the UPC of lead nuclei. Starting from the one-photon excitation mechanism, the total cross section depends on the flux of photons in a nucleus and photon absorptive cross section [5]:

$$\sigma(PbPb \xrightarrow{1\gamma} PbPb^*) = \int \int \sigma_{abs}(E_\gamma) N(E_\gamma, b) d^2b dE_\gamma. \quad (3)$$

Here $N(E_\gamma, b)$ is photon flux associated with ultrarelativistic nucleus (see e.g. [12] and Fig. 1). Rather, a broad range of energy and impact parameter are necessary to calculate the integral precisely. Please note that for large b one has $\vec{b} \approx \vec{b}_1$ or $\vec{b} \approx \vec{b}_2$ for single nucleus excitation. Here, by \vec{b}_1 or \vec{b}_2 , we understand the transverse distance of the photon (interaction point) from nucleus 1 or nucleus 2, respectively, so-called photon impact parameter.

$$\sigma(PbPb \xrightarrow{1\gamma 1\gamma} Pb^*Pb^*) = \int P_{A_1}(b) P_{A_2}(b) d^2b, \quad (4)$$

where

$$P_{A_i}(b) = \int \sigma_{abs}(E_\gamma) N(E_\gamma, b) dE_\gamma. \quad (5)$$

¹ The RELDIS code is not accessible to us.

TABLE I: Cross section σ_{tot} [b] for generating a given number of neutrons in UPC for $\sqrt{s_{NN}} = 5.02$ TeV, for different values of E_0 parameter of the step-like TCM confronted with pure GEMINI++ and TCM with sin-like function predictions. In bold we show results for $E_0 = 50$ MeV. This value will be used throughout this paper.

<div style="display: inline-block; transform: rotate(-45deg);"> E_0 [MeV] kn </div>	σ [b]								
	ALICE [2]	RELDIS	GEMINI++	TCM					
	experiment			sin-like	step-like				
				50	30	40	50	60	70
1	108.4±3.90	104.1± 5.2	93.71	83.37	99.39	99.06	98.75	98.47	98.22
2	25.0±1.30	21.9± 1.1	25.06	21.16	23.51	24.77	25.55	26.05	26.38
3	7.95±0.25	7.59± 0.38	3.05	4.05	5.91	6.02	6.07	6.06	6.02
4	5.65±0.33	4.29± 0.22	2.32	4.19	6.22	6.30	6.32	6.30	6.34
5	4.54±0.44	2.95 ± 0.15	1.51	3.42	4.84	4.90	4.91	4.88	4.83

In our previous approach, Ref. [5], we implicitly assumed

$$P(E_{exc}; E_\gamma) \propto \delta(E_{exc} - E_\gamma) , \quad (6)$$

where δ is the Dirac delta function. Above $P(E_{exc}; E_\gamma)$ can be interpreted as a probability of populating equilibrated compound nucleus with a given excitation energy E_{exc} in a process initiated by the photon with energy E_γ . It must be constructed to fulfill the following probabilistic relation:

$$\int_0^{E_\gamma} P(E_{exc}; E_\gamma) dE_{exc} = 1 . \quad (7)$$

This relation can be generalized for a given number (k) of emitted neutrons. The agreement with the data for $k = 1, 2$ neutrons means that at small excitation energies $E_{exc} < 30$ MeV, where the GDR mechanism dominates [5], the whole photon energy is absorbed by the nucleus. The deexcitation of the Pb nucleus is done with the GEMINI++ program [7] which provides all information about γ -rays emission, various particle evaporation and fission in wide energy excitation range.

The situation changes for larger excitation energies where not the whole photon energy goes to the production of a equilibrated compound nucleus.

The energy could be dissipated in the pre-equilibrium emission of particles such as neutrons, protons or pions, the reactions of quasi-deuteron [24] or other processes.

In our TCM the E_{exc} is typically smaller than the photon energy E_γ . This was established already in $\gamma + A$ collisions [6]. At small energies where giant dipole resonance is excited: $E_{exc} \approx E_\gamma$. Here the Compton scattering is also possible in principle [25]. At larger energies only a part of energy is transferred to the equilibrated system (see also [15]). This fact starts clearly at energy where reactions on quasi-deuteron (or correlated pn pair in another language) become dominant. This means that already at these energies we have preequilibrium processes. One (or even two) of the constituents of the pn pair may escape before equilibration. At higher

energies the situation is less obvious and the notion of preequilibrium is defined somewhat worse. The details depend on a particular dynamical model. For energies $E_\gamma < 140$ MeV one preequilibrium neutron may be a realistic case. Our model was inspired by the presence of quasi-deuteron mechanism. However, we will use it also for energies $E_\gamma > 140$ MeV.

In order to better understand the situation, we consider a simple model in which different excitation energies $E_{exc} < E_\gamma$ can be populated. We started with the somewhat academic step-like function:

$$P(E_{exc}; E_\gamma) = \text{const}(E_{exc}) = 1/E_\gamma \quad (8)$$

for $E_{exc} < E_\gamma$, i.e. uniform population in excitation energy.

Another option is to take the simple sinus-like function:

$$P(E_{exc}; E_\gamma) = \frac{\pi}{2E_\gamma} \sin(\pi E_{exc}/E_\gamma) \quad (9)$$

for $E_{exc} < E_\gamma$.

A comparison of the results with the two excitation functions will be instructive.

The following results for the interpretation of the excitation energy from the initial energy of the interacting photons are obtained with the two-component model (TCM), where delta-like and step-like or sinus-like functions are combined.

In general, the bigger number of neutrons, the larger the fraction of energy carried by neutrons.

$$P(E_{exc}; E_\gamma) = c_1(E_\gamma)\delta(E_{exc} - E_\gamma) + c_2(E_\gamma)/E_\gamma . \quad (10)$$

The probabilistic interpretation requires:

$$c_1(E_\gamma) + c_2(E_\gamma) = 1 . \quad (11)$$

In general, c_1 and c_2 may (should) depend on photon energy E_γ . As a trial function for further analysis, we propose

$$c_1(E_\gamma) = \exp(-E_\gamma/E_0) , \quad (12)$$

$$c_2(E_\gamma) = 1 - \exp(-E_\gamma/E_0) . \quad (13)$$

The parameter E_0 can be adjusted to the ALICE data [2]. We suggest $E_0 \approx 50$ MeV to start with.

The full TCM formula for the probability of emitting a specified number of neutrons for a given photon energy is calculated by:

$$P_k(E_\gamma) = \sum_{E_{exc}}^{E_\gamma} (1 - \exp(-E_\gamma/E_0)) \frac{1}{E_\gamma} \frac{N_k(E_{exc})}{N_{ev}} \Delta E_{exc} + \exp(-E_\gamma/E_0) \frac{N_k(E_\gamma)}{N_{ev}}. \quad (14)$$

Here, the $N_k(E)$ is a number of events with k emitted neutrons for a given E_γ or an excitation energy, and N_{ev} is a total number of events for a given energy. Both numbers are obtained from GEMINI++ event generator. The ΔE_{exc} is a chosen interval of excitation energy in a discrete sum in Eq. 14. This is purely technical parameter to simplify the calculations. The neutron emission probability fulfill the following condition:

$$\sum_k P_k(E_\gamma) = 1. \quad (15)$$

The formula (14) contains a free parameter E_0 , which was fitted to reproduce the dependence of the excitation energy of Pb on the photon energy beam. Authors of [26] displayed the dependence of the excitation energy on the photon energy using the cascade-evaporation model tuned to reproduce the data on fissilities of nuclei at intermediate energy.

In Table I we show cross sections for the emission of various number of neutrons for different values of E_0 parameter. The resulting cross sections for a given number of neutron emissions ($n = 1, 2, 3, 4, 5$) only weakly depend on the value of the phenomenological parameter. Therefore in the following when referring to the TCM we will show results for $E_0 = 50$ MeV as representative. The bigger E_0 the higher cross section for emission of 2, 3, 4, 5 neutrons. On the contrary, the emission of single neutron decreases with increasing E_0 . The result for the sin-like function seems to be worse than the results for the step-like formula. For comparison we display result for the pure GEMINI++ approach where $E_\gamma = E_{exc}$. The pure GEMINI++ approach fails to describe the new ALICE data for neutron multiplicity bigger than 2. Other more realistic functions can be proposed.

D. Pre-equilibrium emission estimation

Nuclei interacting with photons with energy less than (25 – 30) MeV usually deexcite by neutron or γ -rays emission including the Giant Dipole Resonances. In this case all photon energy is transformed into excitation energy of the nucleus. For more energetic photons (30 – 140) MeV,

the equilibration stage is long enough to open also the possibility of the emission of the particles before thermalization of the nucleus. In such a case, a part of the incident energy is lost by neutron or/and proton emission, and the main deexcitation process starts from a somewhat smaller nucleus than the initial colliding one.

In the moderate energy regime, below the particle production threshold, there exist some theoretical estimation how much energy can be used for the pre-equilibrium stage.

The photon energy regime above 140 MeV is connected with the highly energetic particles production such as pions, muons and it is quite well described, e.g. by the GiBUU model [27].

In the review of Pshenichnov et al. [15], the results of the RELDIS model are presented. The author explains the difference between the excitation and incident energies by the pre-equilibrium emission of the particles.

This assumption encourage our study on the estimation of the amount of the particles lost by the nucleus during thermalization process. Thus in place of TCM one can try to use another realistic predictions of the particles emitted before the energy equilibration of nucleons inside the excited nucleus occurs. One of the possibility is to employ the well-known collisions models relevant for particle+nucleus collisions such as Heavy Ion Phase-Space Exploration (HIPSE) [10].

The HIPSE model describes the heavy-ion collision in several stages: from the contact point, by reaggregation of the particles coming from overlapping nuclei till deexcitation of the thermalized prefragment. This last stage is done within the state-of-art statistical approach GEMINI++. In general, it was used with success to describe reaction with collision energies 15 – 100 MeV/nucleon. For the sake of this study, the reaction $n + {}^{207}\text{Pb}$ is chosen, as the neutron interactions should be the best possible approximation of the photon interaction one can do.²

Fig. 3 allows to estimate how much energy is dissipated into internal degrees of freedom in various models. Previous excitation energy estimations were done with the help of intranuclear cascade to describe experimental photofission cross sections, for Bi and Au nuclei [26] and also average multiplicities of neutrons, protons and pions for Pb and U [17] in photon energy range 0.05-1.0 GeV. The HIPSE calculation gives a similar trend. The average excitation energy in TCM with step-like function can be approximated as:

$$\langle E_{exc} \rangle = c_1(E_\gamma) \cdot E_\gamma + c_2(E_\gamma) \cdot \frac{E_\gamma}{2}. \quad (16)$$

The photon of 100 MeV energy excites the Pb nucleus mostly to 40 MeV and the rest is lost on emission of pre-equilibrium particles and internal rearranging of the nucleons inside the hit nucleus. The shadowed area shows

² The HIPSE does not allow for $\gamma + A$ collisions.

the results of fitting E_0 parameter (Eq. (12, 13)) and in average the $E_0 = 50$ MeV gives the best reproduction of data from previous calculation [26]. Thus, this value is taken to further investigation.

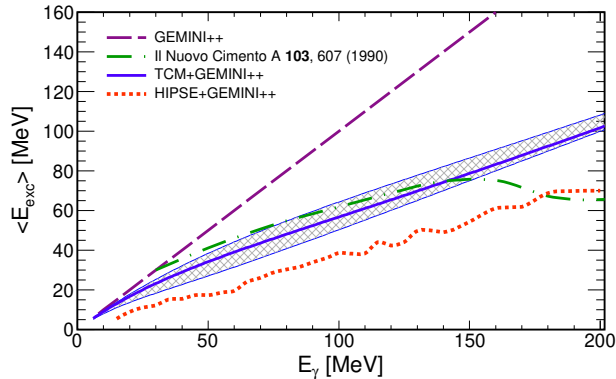


FIG. 3: Dependence of excitation energy of ^{208}Pb ion as a function of photon energy. The Monte Carlo CASCADE simulation [26] (green), the TCM (blue), GEMINI++ (purple) and HIPSE+GEMINI++ (red). The shadowed area shows results of TCM with $E_0 \in (20, 80)$ MeV.

The difference between neutron and photon-induced reactions are displayed in Fig. 3. The Guaraldo et al. [26], the TCM and the HIPSE models estimations of excitation energy show that the energy dissipation ($E_\gamma - E_{exc}$) in the case of the neutron-induced reaction can increase up to 80 MeV for $E_\gamma = 150$ MeV in comparison to photon-induced one, where it is around 60 MeV. This is also well visible in the case of the mean neutron multiplicity presented in Fig. 4. The experimental points were extracted from a measurement of photon-induced neutron emission [6]. The average number of neutrons is still within the experimental uncertainty but missing around 2 neutrons in the case of HIPSE+GEMINI++. Thus these event generator estimations give only the lower limit of the amount of particles lost during the process of equilibration of an excitation energy between nucleons inside the colliding nucleus.

The performance of the TCM average multiplicity is much better, which is obvious as the function has been fitted to the previously checked dependence of excitation energies. Despite this small inconsistencies, the HIPSE allows to verify the statement that for reaction with photon energies larger than 30 MeV, the pre-equilibrium emission is very important. The maximal number of neutrons emitted during one event changes from 0.9 for $E_\gamma = 30$ MeV up to 11 for $E_\gamma = 140$ MeV, thus this is the minimal amount of particles which the initial nucleus loses during the energy equilibration stage.

In general, not only neutrons are evaporated. Fig. 5 shows the distribution of the charge of the prefragments left after the equilibration stage. The initial ^{208}Pb emits up to 10 nucleons for $E_\gamma > 100$ MeV. For low-energy reaction, there are mainly neutron and proton evaporation channels opened, but for 140 MeV incident energy even,

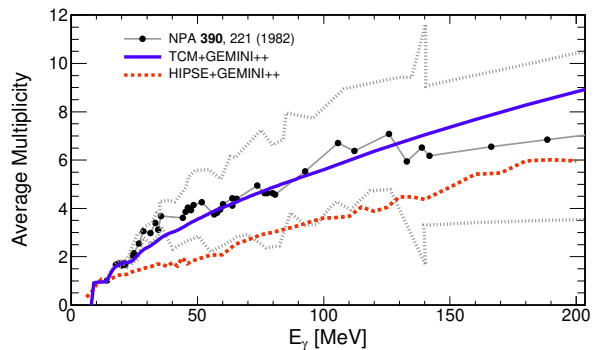


FIG. 4: The mean neutron multiplicity: experimental [28] (black) and estimated with TCM (blue) and HIPSE model (red). The grey dotted lines show the experimental uncertainty.

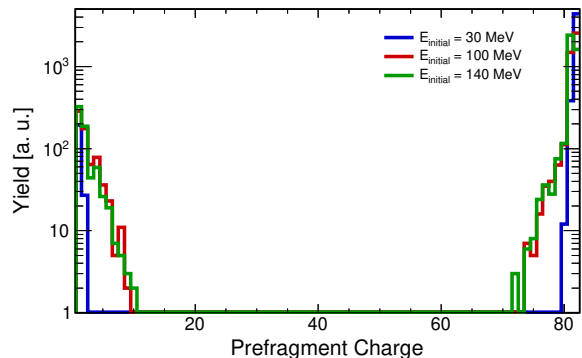


FIG. 5: The prefragment charge distribution calculated with the HIPSE model for neutron incident energy 30, 100 and 140 MeV.

isotopes of carbon and oxygen could reduce the charge of the initial lead nucleus.

The present studies may also be important for a better understanding of the electromagnetic interaction between the spectator and particles produced in the participant zone [29, 30].

It is quite surprising that even for the ultraperipheral collision the charge of the nucleus can differ by as many as 10 units (Fig. 5), thus in the case of lead nuclei, there is a full ensemble of species produced down to Ytterbium. Of course, such cases have a low probability but still it has to be taken into consideration.

Moreover, the predicted excitation energy for a given incident energy (i.e. $E_{initial} = 100$ MeV in Fig. 6) is distributed in full range and depends on the mass and charge of the prefragments. The emitted particles could carry away kinetic energy in addition to the energy needed to separate them from the excited nucleus.

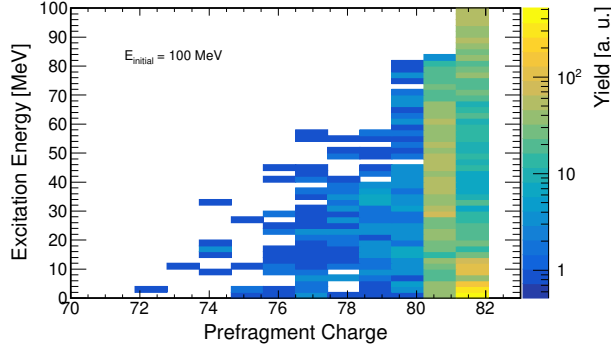


FIG. 6: The distribution of the excitation energy of the prefragment charges calculated with the HIPSE model for neutron incident energy 100 MeV.

E. Compound nucleus deexcitation

The deexcitation of the hot nucleus at moderate excitation energy can be described by many statistical and dynamical models. In the present studies the state-of-art statistical model GEMINI++ [7] was employed as it gives very reasonable results in the investigated energy regime. Moreover, in the past, it was used to discuss the Giant Dipole Resonance emission from the photon-induced Pb collision below 30 MeV [5]. As the GEMINI++ doesn't depend on the way of producing hot nuclei, but only on the initial excitation energy, spin, mass and charge are important, it can be also used as an afterburner.

The evaporation process in the GEMINI++ statistical code [7, 31] is described by the Hauser-Feshbach formalism [8], in which the decay width (in MeV) for the evaporation of an i -th particle from the compound nucleus, with an excitation energy of E^* and spin s_{CN} , is given by the expression

$$\Gamma_i = \frac{1}{2\pi\rho(E^*, s_{CN})} \times \int d\epsilon \sum_{s_d=0}^{\infty} \sum_{J=|s_{CN}-s_d|}^{s_{CN}+s_d} \sum_{\ell=|J-s_i|}^{J+s_i} T_\ell(\epsilon) \rho(E^* - B_i - \epsilon, s_d). \quad (17)$$

Above: s_d is the spin of the daughter nucleus, while s_i , J , and ℓ are, respectively, the spin, total angular momentum, and orbital angular momentum of the evaporated particle, ϵ and B_i are the kinetic and separation energies, T_ℓ are the transmission coefficients, and ρ and ρ_{CN} are the level densities of the daughter and compound nuclei. They have been calculated using the expression taken from [7]:

$$\rho(U, s) = \frac{(2s+1)}{24\sqrt{2}(1+U^{5/4}\sigma^3)^4\sqrt{a(U, s)}} \times \exp(2\sqrt{a(U, s)U}), \quad (18)$$

where $\sigma = \sqrt{\mathcal{J}T}$, with \mathcal{J} being a moment of inertia of a rigid body with the same density as the nucleus. In this

context, T is the nuclear temperature defined as:

$$\frac{1}{T} = \frac{dS}{dU}, \quad \leftrightarrow \quad S = 2\sqrt{a(U, s)U}, \quad (19)$$

where S represents the nuclear entropy, and where thermal excitation energy U is calculated with taking into account both, pairing δP and the shell corrections δW :

$$U = E^* - E_{\text{rot}}(s) + \delta P + \delta W. \quad (20)$$

Here, $E_{\text{rot}}(s)$ stands for the rotational energy of the nucleus.

The level density parameter $a(U, s)$ was parametrized after Ref. [7] as

$$a(U, s) = \tilde{a}(U) \left(1 - h(U/\eta + s/s_\eta) \frac{\delta W}{U} \right), \quad (21)$$

where δW is the shell correction to the liquid-drop mass and \tilde{a} is the smoothed level-density parameter (see below). The separation energies B_i , nuclear masses, shell and pairing corrections were taken from Ref. [32]. The function specifying the rate of hindrance is $h(x) = \tanh x$, with damping parameters $\eta = 18.52$ and $s_\eta = 50\hbar$ [7].

Level density parameter $\tilde{a}(U)$ depends on the excitation energy:

$$\tilde{a}(U) = \frac{A}{k_\infty - (k_\infty - k_0) \exp\left(-\frac{\kappa}{k_\infty - k_0} \frac{U}{A}\right)}, \quad (22)$$

with parameters: $k_0 = 7.3$ MeV, $k_\infty = 12$ MeV and $\kappa = 0.00517 \exp(0.0345A)$ [7].

Within the Monte Carlo GEMINI++ calculations we assume that the excited nucleus was formed with angular momentum equal to $0\hbar$ (which is a good approximation for photon-induced reaction) and its excitation energy which was probed with 2 MeV step for energies below 100 MeV and with 20 MeV step for above 100 MeV value (with generated 10^6 events per every excitation energy).

F. Model results

The present investigation compares four scenarios:

- (1) The pure GEMINI++ assuming $E_{exc} = E_\gamma$;
- (2) The GEMINI++ results weighted by the Dirac delta + step-like functions (TCM) which nicely reproduces previous theoretical and experimental results of [26, 33];
- (3) The hybrid model, where the collision part is described by n+Pb reactions within HIPSE event generator and next cooled down with GEMINI++;
- (4) EMPIRE - Nuclear Reaction Model Code System for Data Evaluation [11] - set of nuclear models which permits to calculate various nuclear reaction in a broad range of beam energies.

Fig. 7 gives the idea about the mean multiplicity of neutrons, protons and alpha particles, emitted during the

whole process. It is obvious that neutrons are the most favorable channel of deexcitation but still some numbers of protons and alphas but also deuterons, tritons and other light charged particles could be detected.

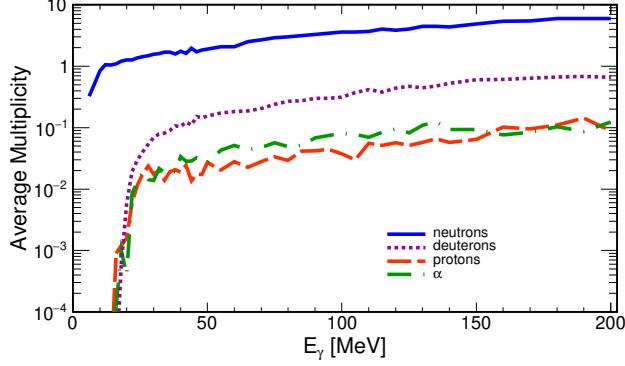


FIG. 7: The average multiplicity of the neutron, proton, deuteron and α particle emitted during the full process (including pre-equilibrium stage) calculated with HIPSE + GEMINI++ hybrid model.

The measurements of a given number of neutrons coming from deexcitation of photon-induced excitation of Pb in the E_γ energy range (30 – 140) MeV are very seldom. A set of articles on this subject was presented by Lepretre et al. in the early nineties [28, 33]. In their experiments the total nuclear absorption cross section for Sn, Ce, Ta, Pb and U was obtained using a monochromatic photon beam. The experimental data for given neutron numbers shown in Fig. 8 are extracted from a Fig. 2 in Ref. [33], where so-called cumulative results were shown.

Assuming that the full photon energy is transformed into excitation of ^{208}Pb the full line shows pure GEMINI++ neutron energy spectra in Fig. 8 which reproduces nicely the low energy bump in cross section for each neutron number distribution but is missing the high energy tails. The TCM + GEMINI++ (dashed line) and HIPSE + GEMINI++ (dotted line) reproduce high E_γ the tails but HIPSE underestimates the low energy neutron production.

In the first approach we assume that the whole photon energy is absorbed by the second (absorbing) nucleus i.e. $E_{exc} = E_\gamma$ and assume equilibrium. Then, the emission of neutrons is given by a cascade of the Hauser-Feshbach emissions as implemented in the well-known code GEMINI++ [7].

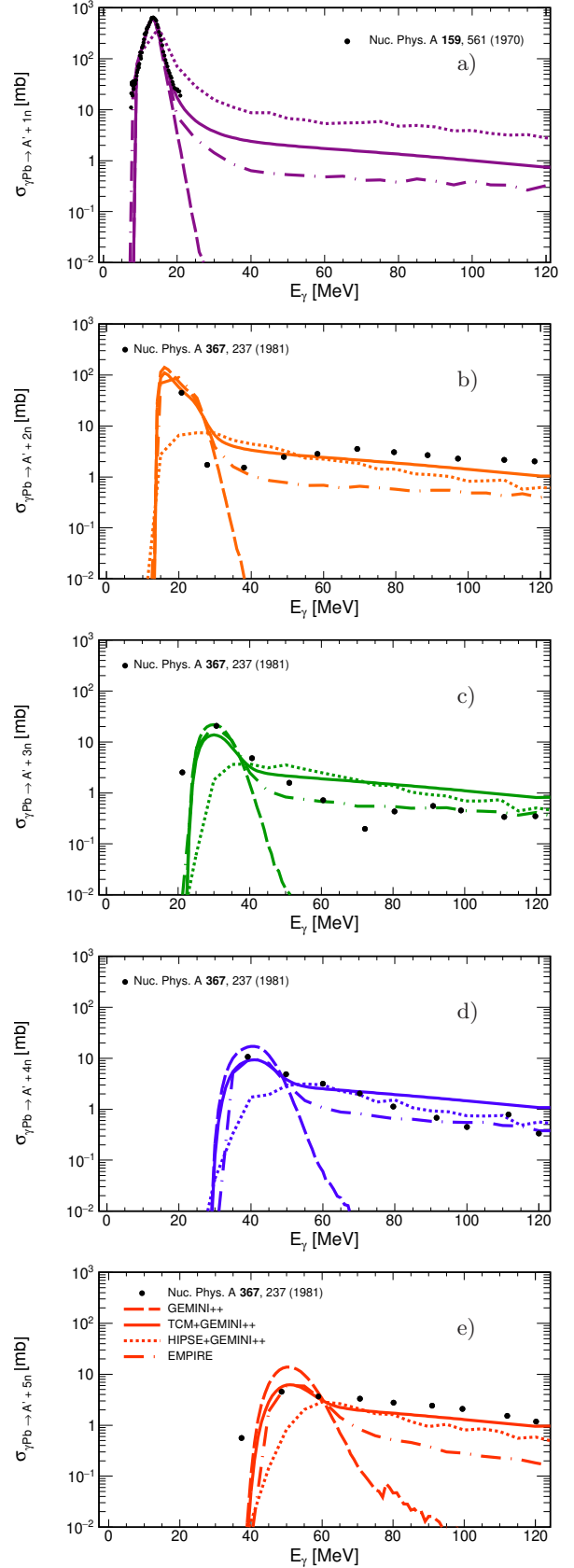


FIG. 8: The cross section for the $\gamma + ^{208}\text{Pb} \rightarrow kn + X$ reaction, where are displayed neutron multiplicities: $k=1$ (a), $k=2$ (b), $k=3$ (c), $k=4$ (d) and $k=5$ (e). We compare results of experimental data from [33] (dots) with model calculations: pure GEMINI++ (dashed line), TCM+GEMINI++ (solid line), HIPSE+GEMINI++ (dotted line) and EMPIRE (dash-dotted line). The color coding here will be used in the rest of the paper.

The best data reproduction was obtained by EMPIRE [11] calculations. This is due to the fact that EMPIRE combines many different nuclear models suited to correctly describe the specific phenomena and fit some selected experimental data.

The photon-induced reaction calculation includes the initial photo-nuclear excitation process, subsequent decay of the excited nucleus by particle and γ -ray emission. The Giant Dipole Resonance and photo-absorption on a neutron-proton pair (a quasi-deuteron) are also taken into account. The Hauser-Feshbach theory is used for describing the sequential decay of hot nuclei similar to the GEMINI++ approach.

III. NEUTRON EMISSION AT HIGHER PHOTON ENERGIES

In our calculations we use γA photoabsorption cross section as parametrized in [5]. As a consequence, for $\sqrt{s_{NN}} = 5.02$ TeV we get single-photon dissociation cross section $\sigma_{ED} = 210.4$ b. This is similar to the estimation in [4]. It was already recognized in Ref. [4] that the integration must be done up to very high photon energies.

If $E_\gamma > 140$ MeV the situation changes again as nonnucleonic degrees of freedom (nucleon resonances, partons) must enter the game. Here the intra-nuclear hadronic cascade model(s) (see e.g. [34–37]) seem to be more appropriate than nuclear neutron evaporation of the Hauser-Feshbach type discussed in the previous section.³ Most of the INC codes are written rather for hadron-nucleus interactions and not for photon-nucleus interaction. The photon-nucleus interactions are, however, slightly different and, in principle, require a dedicated implementation.

In general, the Eq. (3) can be developed to obtain the cross section for production of neutrons in UPC in one-photon exchange approximation as follow:

$$\sigma_{AA \rightarrow AA' + kn} = \int d^2 b_1 dE_\gamma \sigma_{\gamma+A \rightarrow kn+A'}(E_\gamma) W_1(b) \frac{dN}{d^2 b_1 dE_\gamma}. \quad (23)$$

Above $\sigma_{\gamma+A \rightarrow kn+X}$ is the cross section for inclusive emission of k neutrons, i.e. is integrated over directions of each of the emitted k neutrons. $W_i(b) \approx \frac{\exp(-m(b))}{i!}$ is the weight factor obtained for $m(b)$ - average number of absorbed photons [15]. In [21] those cross sections are taken directly from experimental data (see e.g. [39]) and extrapolated to high energies assuming constant (photon energy independent) cross section. The experimental data are limited to $E_\gamma < 140$ MeV. Is this extrapolation to higher E_γ supported by the underlying dynamics? What is the underlying dynamics?

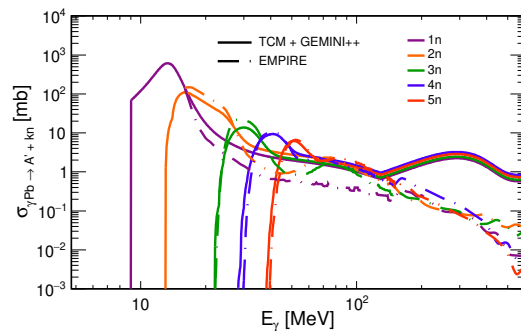


FIG. 9: Cross section for $\gamma + {}^{208}\text{Pb} \rightarrow kn + A'$ as a function of photon energy. The solid line is for our TCM ($E_0 = 50$ MeV) with constant probabilities P_k above $E_\gamma = 200$ MeV. One may clearly see the presence of the Δ resonance at $E_\gamma \approx 200$ MeV which is the desired feature of our approach. For comparison (dashed lines) we show similar results from the EMPIRE code.

The multiplicity dependent cross section

$$\sum_{k=0}^{N_{max}} \sigma_{\gamma+A \rightarrow kn+A'}(E_\gamma) \approx \sigma_{\gamma+A}^{tot}(E_\gamma). \quad (24)$$

Somewhat formally one can write each term in k , corresponding to the emissions of k neutrons, as:

$$\sigma_{\gamma+A \rightarrow kn+A'}(E_\gamma) = \sigma_{\gamma+A}^{tot}(E_\gamma) P_k(E_\gamma). \quad (25)$$

Alternatively one can therefore parametrize $P_k(E_\gamma)$ function to include tails at large E_γ . We do not have, however, reliable predictions as a high-energy $\gamma + {}^{208}\text{Pb} \rightarrow kn + A'$ was not studied experimentally. As a simplest “solution” we assume $P_k(E_\gamma)$ function to be a constant in E_γ . A better approach would be an explicit dynamical model. One possibility would be to use the GiBUU transport approach [27]. The calculation in [40] shows that for large energies of quasi-real photons both small ($M_n < 5$) and large ($M_n > 10$) neutron multiplicities are possible (see Fig. 4 there). Even at large energies the cross section for the emission of a small number of neutrons stays large.

In Fig. 9 we show the cross section for $\gamma + {}^{208}\text{Pb} \rightarrow kn + X$ as a function of the photon energy, from the threshold (a few MeV) to 500 MeV, for different multiplicity of neutrons. The results of the EMPIRE code [11] (short dashed lines) are compared with our TCM extrapolation with constant $P_k(E_\gamma)$ (solid lines). Above $E_\gamma > 140$ MeV the two approaches diverge. Our TCM with constant P_k shows a maximum at $E_\gamma \sim (300 - 400)$ MeV which is due to excitation of nucleon resonances, mostly Δ isobars.

The higher energies, especially in the region of partonic excitations, require further theoretical studies in future. There was some discussion on high-energy scattering of photons on nuclei within dual parton model in [23, 41]. According to our knowledge, no neutron emission was studied in this context.

³ Even at low energies the standard neutron evaporation is modified by the reactions on quasi-deuteron [38].

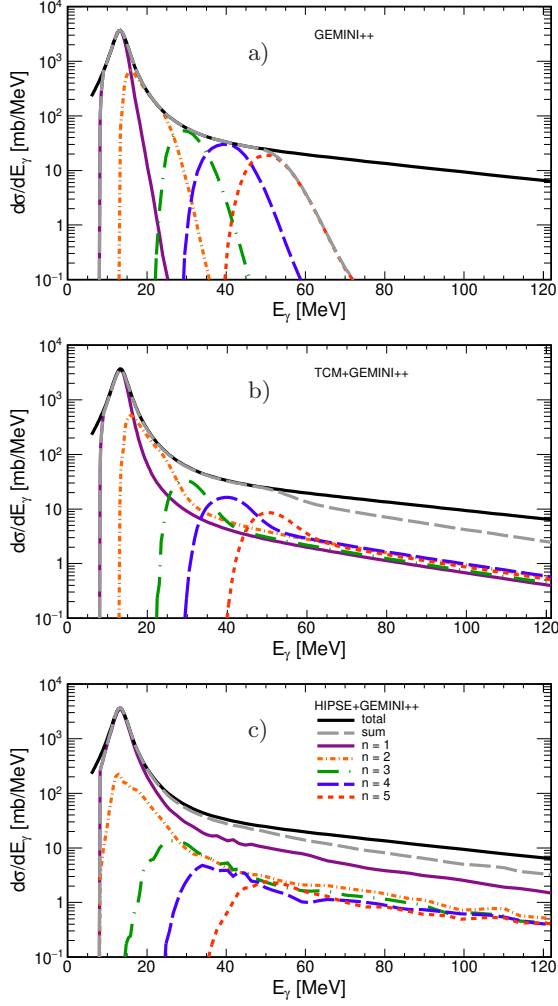


FIG. 10: E_γ distribution for a fixed number of neutron emissions for UPC with energy $\sqrt{s_{NN}} = 5.02$ TeV calculated via (a) GEMINI++, (b) TCM+GEMINI++ and (c) HIPSE+GEMINI++. The solid black line is obtained from Eq. (3) while the sum of up to 5 neutron contributions by the dashed line.

What are photon energies responsible for emission of 1-5 neutrons is a crucial dynamical problem which we approach here in a very phenomenological way.

The outcome of Eq. (23) is displayed in Fig. 10 where the distribution of 1, 2, 3, 4 and 5 neutron emissions as a function of photon energy is shown. The black line marks the total cross section for neutron emission. Fig. 10(a) is for pure Hauser-Feshbach approach as encoded in GEMINI++, Fig. 10(b) relates to the TCM approach and Fig. 10(c) to HIPSE+GEMINI++ model.

In Fig. 11 we present an integrated cross section for $^{208}\text{Pb} + ^{208}\text{Pb} \rightarrow AA' + kn$ as a function of numbers of emitted neutrons (k) for different, somewhat arbitrary, conditions on high photon energies. In panel a) we discuss how the cross section depends on the lowest point where P_k are set to constants. In this case the upper integration limit is set to $E_\gamma^{max} = 2 \cdot 10^8$ MeV. In panel

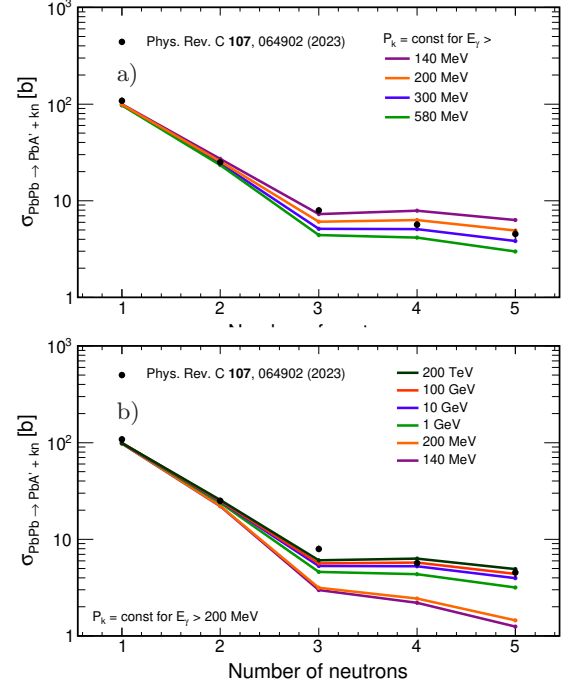


FIG. 11: Cross section for emission of a number of neutrons for different upper limits on E_γ . In panel a) the constant value of P_k starts for changing value given in the panel. The upper limit is very high. In panel b) the P_k constant value starts for $E_\gamma = 200$ MeV. The upper limit is modified to the values shown in the panel.

b) we test the dependence of the cross sections on the upper integration limit E_γ^{max} . In this case the constant values of P_k are set to those for $P_k(E_\gamma = 200 \text{ MeV})$ calculated in our TCM. The excitation energy of ^{208}Pb for $E_\gamma = 200$ MeV is around 100 MeV. In Ref. [42] the fission probability for nearby ^{200}Pb at $E_{exc} \approx 100$ MeV is almost 30% thus the evaporation channel is damped. Moreover, testing various energy cut in our approach these values gave the lowest χ^2 values when comparing to the ALICE data [2].

The cross sections for $^{208}\text{Pb} + ^{208}\text{Pb} \rightarrow AA' + kn$ potentially strongly depend on the high energy (E_γ) behavior of the $\gamma + ^{208}\text{Pb} \rightarrow kn + A'$ cross section. A good description of the ALICE data can be obtained assuming that the region of high- E_γ ($E_\gamma < 100$ GeV) plays a crucial role in production of up to five neutrons. In our opinion this requires further model studies in the future.

In Fig. 12 we show consequences of the assumption $P_k = \text{const}$ for the cross section $\sum_{k=1}^5 \sigma_{\gamma + ^{208}\text{Pb} \rightarrow kn + A'}(E_\gamma)$ in a very broad range of photon energy. It leads to about 10% of the photoproduction cross section shown for the comparison as the black solid line, up to extremely large photon energies. It is impossible to verify at present how reliable is as no experimental data exist. At high energies the result of our present approach (TCM) is very different than that of EMPIRE.

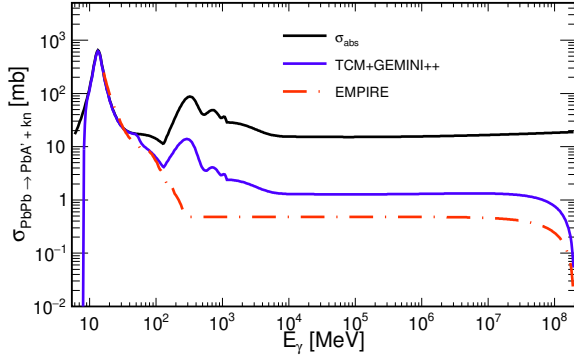


FIG. 12: The sum of cross sections for emitting up to 5 neutrons for TCM+GEMINI++ (blue solid line), EMPIRE (red dash-dot line) and total absorption cross section (black solid line) [4, 33, 43–46].

The tests made above show the uncertainty of our integration, which gives less than 10% of the error. There is also an inaccuracy connected with the number of steps in the integration procedure, but it gives less than 2% for the highest energies. The statistical error is very small as GEMINI++ runs for 10^6 events and HIPSE generates $5 \cdot 10^3$ events.

IV. A NEW PRESCRIPTION FOR MULTIPLE PHOTON EXCHANGES

In this section, we calculate cross section for a given number of neutrons including the exchange of one and multiple photons. We use a formalism discussed partly in [15]. We explicitly include up to 4 photon exchanges.

The simplest model (one photon exchange + equilibrium) is almost right for one and two neutron emissions (Table II) but does not describe in detail the emission of 3, 4, 5 neutrons. In Table II results for single photon exciting single nucleus are displayed and compared with experimental data from the ALICE Pb+Pb ultraperipheral collisions at energy 5.02 TeV [2]. Pure GEMINI++ for $k=3, 4, 5n$ gives the lowest estimation due to the missing contributions from high-energy tails in E_γ spectra. The TCM improves the situation considerably.

Thus we check to which extent multiple photon exchanges, as illustrated in Fig. 13 can be responsible for the clear disagreement with the ALICE data for the number of emitted neutrons $n > 2$. Each additional photon exchange leads, on average, to higher nucleus excitation and, as a consequence, the emission of a bigger number of neutrons. As the 1-photon excitation is the most probable, let's call this process: "leading order" (LO), 2-photon gives smaller correction thus it will be "next-to-leading order" (NLO), 3-photon absorption- "next-to-next-to-leading order" (NLO₂), 4-photon absorption- "next-to-next-to-next-to-leading order" (NLO₃), what is shown in Fig. 13, respectively.

TABLE II: Total cross sections (in barn) for a fixed number of neutron emission in UPC with energy 5.02 TeV. By TCM we mean here Dirac delta + step-like probability function including GEMINI++. Pure GEMINI++ (GEM.), HIPSE+GEMINI++ (HG) and EMPIRE results are also presented. Here, only one photon exchange is taken under consideration (Fig. 13a).

kn	σ [b]			
	GEM.	TCM	EMPIRE	HG
1	93.71	98.75	100.19	122.11
2	25.06	25.55	24.71	15.14
3	3.05	6.07	5.41	4.53
4	2.32	6.32	5.37	3.42
5	1.51	4.91	3.24	3.67

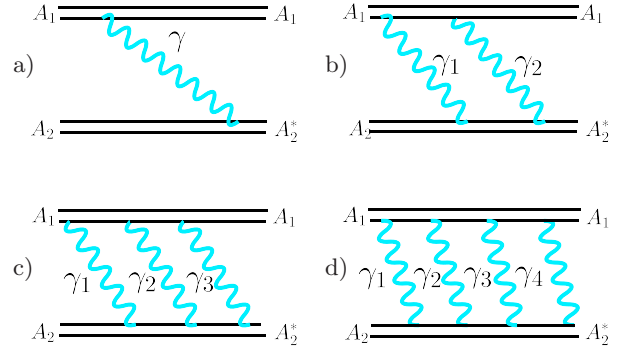


FIG. 13: Photon absorption by single nucleus (A_2). In panel a) one-photon absorption (LO), b) two-photon absorption (NLO), c) three-photon absorption (NLO₂) d) four-photon absorption (NLO₃).

The cross section for k neutron emission from one nucleus in $AA \rightarrow A^*A$ collisions can be formally written as

$$\frac{d\sigma^k}{dE_\gamma} = \sum_{i=1}^4 \frac{d\sigma_i^k}{dE_{\gamma,i}}, \quad (26)$$

where i is the number of photons exchanged (we numerically include up to 4 photons) and

$$\frac{d\sigma_i^k}{dE_{\gamma,i}} = \frac{d\sigma_i}{dE_{\gamma,i}} P_k(E_{exc}), \quad (27)$$

where $P_k(E_{exc})$ is a relative probability to produce k neutrons at excitation energy $E_{exc} = \sum_{i=1}^4 E_{\gamma,i}$. This probability density can be calculated e.g. in the Hauser-Feshbach approach (see Ref.[5]). The $\frac{d\sigma_i}{dE_{exc}}$ contains implicitly weight factors, $W_i(b) \approx \frac{\exp(-m(b))}{i!}$ due to indistinguishable exchange photons to avoid double counting (see, e.g., [15]).

The cross section for i photon absorption by single nucleus in $AA \rightarrow AA^*$ collision can be deduced from Eq. (3)

TABLE III: Cross section for emission of k neutrons via exchange of $i = 1, 2, 3$ and 4 photons for $\sqrt{s_{NN}} = 5.02$ TeV. $E_{exc} = E_\gamma$ approximation and GEMINI++ code are used here.

kn	σ [b]				
	LO	NLO	NLO ₂	NLO ₃	all
1	93.713	0.008	0.000	0.0000	93.721
2	25.057	0.429	0.001	0.0000	25.487
3	3.054	0.385	0.023	0.0000	3.462
4	2.316	0.103	0.080	0.0006	2.499
5	1.505	0.038	0.027	0.0229	1.593

TABLE IV: Cross section for emission of k neutrons via exchange of 1, 2, 3 and 4 photons for $\sqrt{s_{NN}} = 5.02$ TeV. Two-component model TCM ($E_{exc} < E_\gamma$) is used for each exchange as described in the text.

kn	σ [b]				
	LO	NLO	NLO ₂	NLO ₃	all
1	98.749	0.295	0.067	0.0010	99.112
2	25.549	0.637	0.095	0.0014	26.282
3	6.065	0.410	0.084	0.0011	6.560
4	6.324	0.260	0.121	0.0015	6.706
5	4.909	0.191	0.076	0.0013	5.178

and (23):

$$\frac{d\sigma_i}{dE} = \int dE_1 \dots dE_i \delta(E_1 + \dots + E_i - E) N(E_1, b) \dots N(E_i, b) \sigma_{\gamma+A \rightarrow A'}(E_1) \dots \sigma_{\gamma+A \rightarrow A'}(E_i) W_i(b) d^2b. \quad (28)$$

In Table III, we present our result for the cross section for a given number of photon exchanges. The multiphoton exchange processes were studied before in [47], where the independence of the photon emission was discussed. The high energy of the colliding nuclei outbalances the photon energy. In consequence different interactions can be treated independently. The possible effect of correlation of neutrons emitted after mutual GDR excitation discussed e.g. in Baur et al. [47] cannot be observed in high energy collider mode when particles are emitted in very forward directions due to kinematical boost.

Here, for each photon exchange (i), we assume $\delta E_{exc}^{(i)} = E_\gamma^{(i)}$ where δE_{exc} is a part of the excitation due to individual photon exchange. We observe an improvement, e.g. for three neutron emission the model of two-photon exchange enhances the cross section by 10%, but still something is missing.⁴

⁴ Are mutual excitations (simultaneous excitation of both collision partners) important in this context? Two questions are related to this issue. Are mutual excitations eliminated by the way the experimental data of the ALICE collaboration is obtained? Does ALICE require no neutron emission from the second nucleus?

The one photon exchange has a maximum for $1n$ production, the two-photon exchange for $3n$ production, the three photon exchange for $4n$ production. Moreover Fig. 10 shows distribution of excitation energy for a given number of neutrons and exchanged photons which presents our point even better.

In Table IV, we present our result for the different numbers of photon exchanges for the two-component model (TCM) to simulate pre-equilibrium effects. We get the higher-order corrections of the order of 10% for $k=3, 4, 5$.

For completeness in Fig. 14 we present distribution in excitation energy, estimated as a sum of photon energies that hit the single nucleus, for a given number of photons and neutrons using TCM as described in the text above.

V. MUTUAL EXCHANGE OF PHOTONS BETWEEN NUCLEI

Also mutual excitations, understood as simultaneous excitations of both nuclei must be, in principle, included. Some examples of corresponding photon exchanges are shown in Fig. 15.

The corresponding leading-order cross section (diagram (a)) for the mutual excitation, following Eq. (28), (see e.g. [15]) reads:

$$\sigma_{A_1 A_2 \rightarrow A_1^* A_2^*}(E_1, E_2) = \int dE_1 dE_2 d^2b \quad (29)$$

$$N(b, E_1) \sigma_{\gamma+A_2 \rightarrow A_2^*}(E_1) N(b, E_2) \sigma_{\gamma+A_1 \rightarrow A_1^*}(E_2).$$

For example, the cross section for 1 neutron emission from the first excited nucleus A_1^* and 1 neutron emission from the second excited nucleus A_2^* can be then written as

$$\frac{d\sigma_{AA \rightarrow A_1^* A_2^*}}{dE_1 dE_2} = \int d^2b N(b, E_1) P_{1kn}^{1\gamma}(E_1) \sigma_{\gamma+A_1 \rightarrow A_1^*}(E_1) \times N(b, E_2) P_{2kn}^{1\gamma}(E_2) \sigma_{\gamma+A_2 \rightarrow A_2^*}(E_2), \quad (30)$$

where $P_1(E_1)$ and $P_1(E_2)$ are familiar one neutron emission probabilities which have to be modeled, e.g. in the Hauser-Feshbach approach or in TCM.

One can also consider $(n_{\gamma_1}, n_{\gamma_2}) = (1, 2) + (2, 1) + (2, 2) + \dots$ cross sections (see extra columns in Table V) which only slightly improve the agreement with the ALICE data. Here n_{γ_1} is a number of photons emitted by the first and absorbed by the second nucleus.

The cross section for excitation of the first nucleus in mutual interactions reads:

$$\frac{d\sigma_k}{dE_{A_1}} = \sum_l \sum_{i,j} \int dE_{A_2} \frac{d\sigma_{k,l}^{(i,j)}}{dE_{A_1}^{(i)} dE_{A_2}^{(j)}}, \quad (31)$$

where:

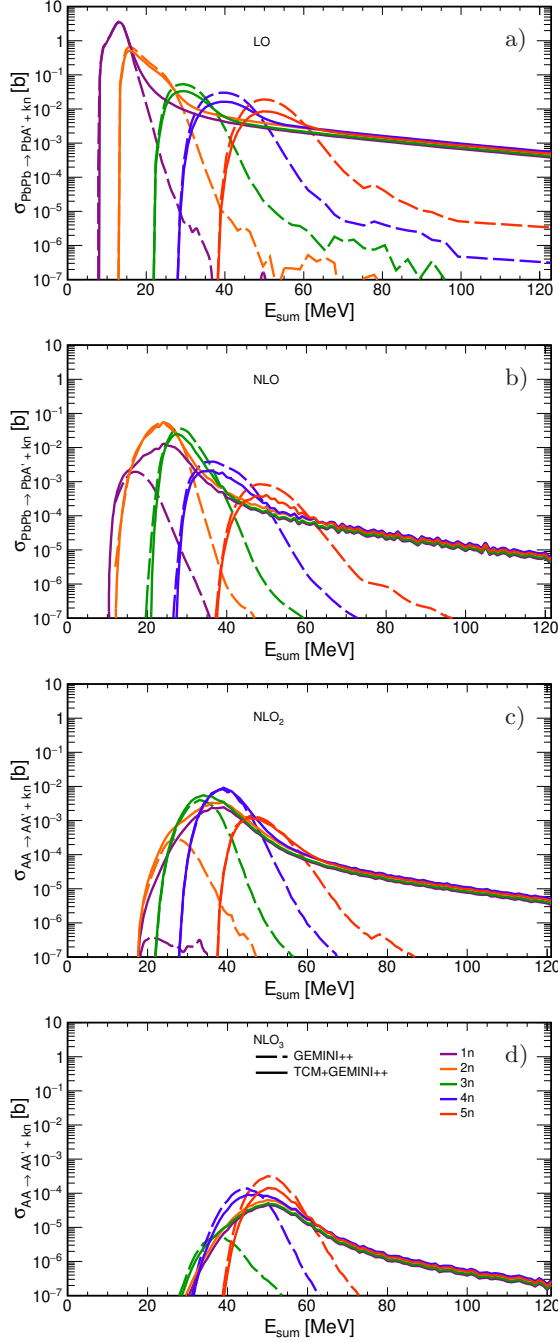


FIG. 14: Distribution in excitation energy for a given number of exchanged photons (a) 1 γ -rays, (b) 2 γ -rays, (c) 3 γ -rays, (d) 4 γ -rays and a given number of emitted neutrons $kn = 1, 2, 3, 4, 5$.

$$E_{A_1}^{(i)} = \sum_{k=1}^i E_{A_1, k}; \quad (32)$$

$$E_{A_2}^{(j)} = \sum_{l=1}^j E_{A_2, l}. \quad (33)$$

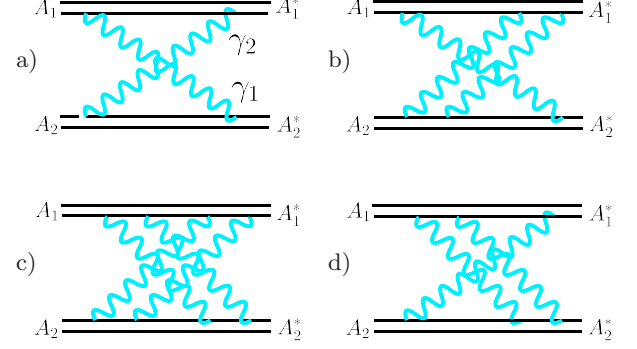


FIG. 15: Multiple photon exchanges - simultaneous excitation of both nuclei, called mutual excitation.

In general, mutual excitations with the same number of exchanged photons are concentrated at smaller impact parameter than single excitations which is due to a bigger number of flux factors involved (for leading order terms one flux factor for single excitation, versus two flux factors for mutual excitation (see Eq.(29))).

The cross sections for mutual excitations are summarized in Table V. These numbers are much smaller than those for single nucleus excitation (see Tables II, III, IV). So mutual excitations cannot explain the discrepancy with the ALICE data. In the mutual excitation also the dominant role plays the exchange of single photons.

A comparison of various components consisting of the final neutron emission cross section is presented in Fig. 16. Logarithmic y-axis can be misleading but allows to show small contributions from 3 and 4 photon exchanges. The biggest influence has the single photon-single nucleus excitation process and other cases are just a correction. However, interesting is the fact that they are almost independent of the number of emitted neutrons.

The Fig. 17 summarizes the observation made in our paper. The effect of pre-equilibrium emission is illustrated by comparison between GEMINI++ and TCF+GEMINI++ or HIPSE+GEMINI++. For emission of higher multiplicity neutrons, important are the high energy photons.

VI. CHARGED PARTICLE EMISSION

The zero degree calorimeter (ZDC) can be used to measure both forward neutrons and protons [48]. Recently the ALICE collaboration presented the first results of the proton measurement in ZDCs [3]. They measured inclusive proton cross section as well as production of selected 1pkn channels with 1 proton and 1, 2, 3 neutrons. The obtained cross section for 1 proton emission is 40.4 b. This can be compared to our results collected in Table VI.

TABLE V: Cross sections in barns for mutual excitations at $\sqrt{s_{NN}} = 5.02$ TeV for a given number of neutrons, assuming full equilibrium in both excited nuclei, i.e. $P_k(E_1)$ and $P_k(E_2)$ are estimated by the TCM.

kn		σ [b]			
		mNLO	mNLO ₂	mNLO ₂	mNLO ₃
A_1, A_2	$1\gamma - 1\gamma$	$1\gamma - 2\gamma$	$2\gamma - 1\gamma$	$2\gamma - 2\gamma$	
1 1	0.2977	0.0264	0.0264	0.0018	
1 2	0.0868	0.0568	0.0077	0.0045	
1 3	0.0262	0.0365	0.0023	0.0022	
1 4	0.0295	0.0232	0.0026	0.0011	
1 5	0.0295	0.0171	0.0021	0.0008	
2 1	0.0868	0.0077	0.0568	0.0045	
2 2	0.0253	0.0166	0.0166	0.0111	
2 3	0.0077	0.0107	0.0051	0.0056	
2 4	0.0086	0.0068	0.0057	0.0030	
2 5	0.0070	0.0050	0.0046	0.0021	
3 1	0.0262	0.0023	0.0365	0.0022	
3 2	0.0077	0.0051	0.0107	0.0056	
3 3	0.0023	0.0032	0.0032	0.0026	
3 4	0.0026	0.0021	0.0037	0.0013	
3 5	0.0021	0.0015	0.0030	0.0009	
4 1	0.0295	0.0026	0.0232	0.0011	
4 2	0.0086	0.0057	0.0068	0.0030	
4 3	0.0026	0.0037	0.0021	0.0013	
4 4	0.0029	0.0023	0.0023	0.0006	
4 5	0.0024	0.0017	0.0019	0.0004	
5 1	0.0239	0.0021	0.0171	0.0008	
5 2	0.0070	0.0046	0.0050	0.0021	
5 3	0.0021	0.0030	0.0015	0.0009	
5 4	0.0024	0.0019	0.0017	0.0004	
5 5	0.0019	0.0014	0.0014	0.0003	

TABLE VI: Total cross sections (in barn) for a charged particle emission in UPC $^{208}\text{Pb}+^{208}\text{Pb}$ with collision energy $\sqrt{s_{NN}} = 5.02$ TeV calculated with pure GEMINI++(GEM.), TCM+GEMINI++ (TCM), HIPSE + GEMINI++(HG) and EMPIRE(EMP). The cross section for exclusive channels of $1p1n$, $1p2n$ and $1p3n$ and also inclusive channels $1pXn$, $1dXn$ and $1\alpha Xn$ are compared with ALICE data (exp.), Ref. [3].

Model	σ [b]					
	1p1n	1p2n	1p3n	1pXn	1dXn	1αXn
GEM.	0	0	0	19.56	6.91	30.66
TCM	0.66	0.92	0.72	16.72	11.42	15.47
HG	9.86	0.82	0.93	28.48	64.02	42.38
EMP.	2.43	2.81	0.23	7.06	2.65	0.28
exp.[3]	1.05±0.07	1.35±0.21	1.58±0.57	40.4±1.7	-	-

In Table VI we also show cross section for the emission of 1 proton correlated with various numbers of neutrons: $k=1, 2, 3$ estimated by pure GEMINI++, two-component model with GEMINI++, HIPSE+GEMINI++ and EM-

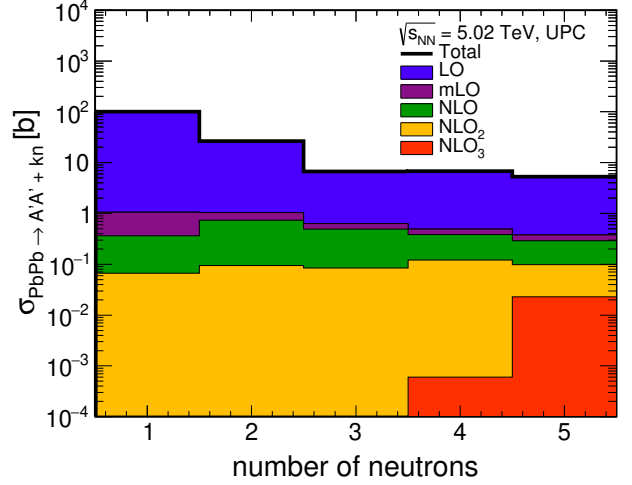


FIG. 16: Various components of the neutron multiplicities cross section from photon-induced Pb nuclei such as: single nucleus-one photon (LO), single nucleus and x+1 photons (NLOx) and both nuclei excited by photons exchange.

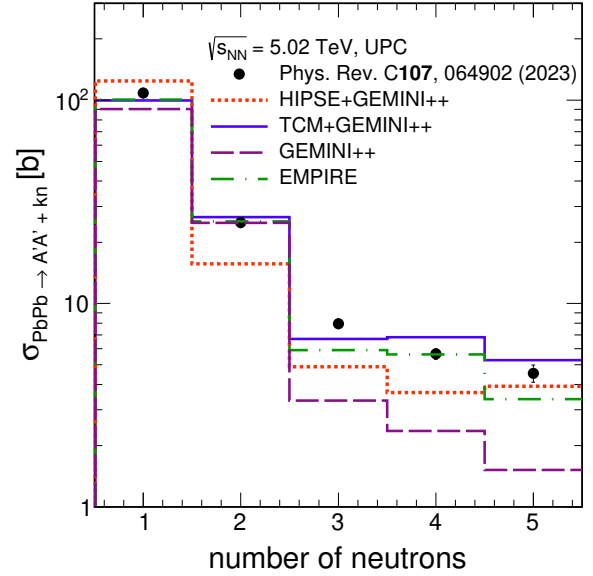


FIG. 17: Total cross section of emission of a given number of neutrons in lead-lead UPC, with collision energy $\sqrt{s_{NN}} = 5.02$ TeV. The dots represent results from the ALICE experiment [9].

PIRE approaches.

In the case of simultaneous emission of protons and a few neutrons, we assumed combined probability to be $P_{ik}^{p,n}(E_\gamma) = P_i^p(E_\gamma)P_k^n(E_\gamma)$.

From GEMINI++ we cannot obtain probability for emission of one proton and one, two or three neutrons due to low proton emission rate in energy range: (10 – 50) MeV. Thus, the zeros for pure GEMINI++ calcu-

lation can be understood as follows: in the Hauser-Feshbach approach, protons are emitted for $E_{exc} > 40$ MeV while 1, 2 and 3 neutron channel are opened for $E_{exc} < 40$ MeV (Fig. 8) i.e. simultaneous emission is not possible. However, integration over all possible 1pXn channels gives meaningful values.

The situation improves for TCM+GEMINI++, where the large tails in E_γ for neutron emission probability $P_k^n(E_\gamma)$ appear.

In general, the EMPIRE platform gives the smallest cross section and the HIPSE+GEMINI++ shows the dominant role of the deuterons in the pre-equilibrium emission.

With the present experimental setting of ZDC, other charged particles than protons are not measured by the proton ZDC. This requires dedicated simulations, including details of the experimental apparatus, which goes beyond the scope of the present paper.

Our numbers seem to be smaller than those measured by the ALICE collaboration. The details depend, however, on the model used. The further theoretical and experimental studies are necessary as the discrepancy between different models is quite significant. We get a reasonable agreement with individual p, n channels.

VII. CONCLUSION

In this paper, we have explored the mechanisms of neutron production in ultrarelativistic, ultraperipheral $^{208}\text{Pb} + ^{208}\text{Pb}$ collisions. In our approach, the Coulomb excitation is calculated as a convolution of photon flux and photoabsorption cross section. The photon flux is calculated in the equivalent photon approximation with approximate or realistic photon fluxes. By realistic, we mean photon flux obtained as a Fourier transform of the realistic charge distribution in ^{208}Pb . The nucleus is excited by the absorption of the exchanged photon. In the previous paper of our group, we assumed $E_{exc} = E_\gamma$. There only a small number of emitted neutrons (up to three) was considered.

Recently, the ALICE collaboration measured up to five neutrons emitted from one nucleus at center-of-mass collision energy $\sqrt{s_{NN}} = 5.02$ TeV. The ALICE collaboration presented cross sections for 1, 2, 3, 4 and 5 neutron production separately. In our approach we have to use a model of emission of particles from the Coulomb excited nucleus. Since typical excitation energies are less than 150 MeV it is natural to assume the Hauser-Feshbach cascade emission as implemented in GEMINI++ program.

We have shown that the sketched above approach is able to describe the larger neutron multiplicity ALICE

data. We have obtained slightly smaller cross sections than the measured ones for neutron multiplicities $M_n > 2$. This has forced us to reconsider some simplifications made in our previous paper and at the initial stage of the present paper.

The approach we have discussed here relies on allowing that not the whole E_γ energy goes to the statistically equilibrated system. Still a part of an energy escapes in the form of pre-equilibrium emissions, which means that E_{exc} of the equilibrated nuclear system is smaller than E_γ in the convolution approach. In this respect, we have proposed a two-component model. One component is treated as previously (full equilibration) but the second component assumes in a hidden way pre-equilibrium emissions. The relative probabilities of each component may naturally depend on E_γ . Such an approach changes cross sections for different neutron multiplicities especially for $k=3, 4, 5$. We have also considered other approaches, such as HIPSE or EMPIRE.

We have discussed the potential role of the high energy photons ($E_\gamma > 140$ MeV) $\gamma + A \rightarrow kn + X$ for small neutron multiplicities relevant for this paper. This issue requires further model studies in the future.

In the first stage, we assumed a single photon exchange. Next, we also included multiple photon exchanges. The latter are more important at larger nuclear excitation, i.e. a bigger number of emitted neutrons. We have reported some improvements.

There can be some other effects which may be responsible for the persisting small disagreement. For example, the measured data may not be fully UPC type; some peripheral collisions may play a difficult to quantify role. Secondly, we have considered simplified formulae for multiple photons exchanges. However, a more refined treatment goes beyond the scope of this paper.

Finally, we have also presented our results for the emission of p, d and α -particles in different nuclear models used in the present studies. At the final stage of this paper new ALICE results for emission of protons became available. Thus we have confronted our estimations with experimental data also for simultaneous emission of protons and neutrons and found fair agreement.

Acknowledgments

We are indebted to Igor Pshenichnov, Krzysztof Pysz, Sergei Ostapchenko, Tanquy Pierog, Wolfgang Schäfer, Daniel Tapia Takaki and Chiara Oppedisano for discussion of topics related to the present paper. This work was partially supported by the Polish National Science Center Grant DEC2021/42/E/ST2/00350.

[1] M. Chiu, A. Denisov, E. Garcia, J. Katzy, and S. N. White, Phys. Rev. Lett. **89**, 012302 (2002), nucl-

ex/0109018.

[2] S. Acharya et al. (ALICE), Phys. Rev. C **107**, 064902

- (2023), 2209.04250.
- [3] S. Acharya et al. (ALICE) (2024), 2411.07058.
 - [4] A. J. Baltz, M. J. Rhoades-Brown, J. Weniger, Phys. Rev. E **54**, 4233 (1996).
 - [5] M. Klusek-Gawenda, M. Ciemala, W. Schäfer, and A. Szczurek, Phys. Rev. C **89**, 054907 (2014), 1311.1938.
 - [6] A. Lepre tre, H. Beil, R. Bergere, P. Carlos, J. Fagot, A. Veyssiere, J. Ahrens, P. Axel, and U. Kneissl, Physics Letters B **79**, 43 (1978), ISSN 0370-2693.
 - [7] R. J. Charity, Phys. Rev. C **82**, 014610 (2010), URL <https://link.aps.org/doi/10.1103/PhysRevC.82.014610>.
 - [8] W. Hauser and H. Feshbach, Phys. Rev. **87**, 366 (1952), URL <https://link.aps.org/doi/10.1103/PhysRev.87.366>.
 - [9] B. Abelev et al. (ALICE), Phys. Rev. Lett. **109**, 252302 (2012), 1203.2436.
 - [10] D. Lacroix, A. Van Lauwe, and D. Durand, Phys. Rev. C **69**, 054604 (2004), URL <https://link.aps.org/doi/10.1103/PhysRevC.69.054604>.
 - [11] M. Herman, R. Capote, B. Carlson, P. Oblozinsk y, M. Sin, A. Trkov, H. Wienke, and V. Zerkin, Nucl. Data Sheets **108**, 2655 (2007).
 - [12] A. J. Baltz, Y. Gorbunov, S. R. Klein, and J. Nystrand, Phys. Rev. C **80**, 044902 (2009), 0907.1214.
 - [13] J. D. Jackson, *Classical Electrodynamics* (Wiley, 1998), ISBN 978-0-471-30932-1.
 - [14] P. Corvisiero, L. Mazzaschi, M. Ripani, M. Anghinolfi, V. I. Mokeev, G. Ricco, M. Taiuti, A. Zucchiatti, Nuc. Instr. and Meth. A **346**, 433 (1994).
 - [15] I. A. Pshenichnov, Physics of Particles and Nuclei **42**, 215 (2011).
 - [16] A.S. Iljanov, I.A. Pshenichnov, N. Bianchi, E.De Sactis, V. Muccifora, M. Mirazita and P. Rossi, Nucl. Phys. A **616**, 575 (1997).
 - [17] V. Barashenkov, F. Gereghi, A. Iljinov, G. Jonsson, and V. Toneev, Nuclear Physics A **231**, 462 (1974), ISSN 0375-9474, URL <https://www.sciencedirect.com/science/article/pii/037594747490540>.
 - [18] J. Ranft (1997).
 - [19] S. Roesler, R. Engel, and J. Ranft, in *Advanced Monte Carlo for Radiation Physics, Particle Transport Simulation and Applications*, edited by A. Kling, F. J. C. Bar o, M. Nakagawa, L. T vora, and P. Vaz (Springer Berlin Heidelberg, Berlin, Heidelberg, 2001), pp. 1033–1038, ISBN 978-3-642-18211-2.
 - [20] S. R. Klein, J. Nystrand, J. Seger, Y. Gorbunov, and J. Butterworth, Comput. Phys. Commun. **212**, 258 (2017), 1607.03838.
 - [21] M. Broz, J.G. Contreras and J.D. Tapia Takaki, Comp. Phys. Commun. **253**, 107181 (2020).
 - [22] W. Chang, E.-C. Aschenauer, M. D. Baker, A. Jentsch, J.-H. Lee, Z. Tu, Z. Yin, and L. Zheng, Phys. Rev. D **106**, 012007 (2022), URL <https://link.aps.org/doi/10.1103/PhysRevD.106.012007>.
 - [23] S. Roesler, R. Engel and J. Ranft, arXiv:9611379 (1996).
 - [24] J. S. Levinger, Phys. Rev. **84**, 43 (1951), URL <https://link.aps.org/doi/10.1103/PhysRev.84.43>.
 - [25] A. Milstein and M. Schumacher, Physics Reports **243**, 183 (1994), ISSN 0370-1573, URL <https://www.sciencedirect.com/science/article/pii/037015739400058>.
 - [26] C. Guaraldo, V. Lucherini, E. De Sanctis, A. Iljinov, M. Mebel, and S. Lo Nigro, Il Nuovo Cimento A **103**, 607 (1990).
 - [27] O. Buss, T. Gaitanos, K. Gallmeister, H. van Hees, M. Kaskulov, O. Lalakulich, A. Larionov, T. Leitner, J. Weil, and U. Mosel, Physics Reports **512**, 1–124 (2012), ISSN 0370-1573, URL <http://dx.doi.org/10.1016/j.physrep.2011.12.001>.
 - [28] A. Lepre tre, H. Beil, R. Berg re, P. Carlos, J. Fagot, A. Veyssiere, and I. Halpern, Nuclear Physics A **390**, 221 (1982), ISSN 0375-9474.
 - [29] K. Mazurek, A. Szczurek, C. Schmitt, and P. N. Nadtochy, Phys. Rev. C **97**, 024604 (2018), URL <https://link.aps.org/doi/10.1103/PhysRevC.97.024604>.
 - [30] K. Mazurek, M. Klusek-Gawenda, and A. Szczurek, Eur. Phys. J. A **58**, 245 (2022), URL <https://doi.org/10.1140/epja/s10050-022-00899-0>.
 - [31] M. Ciemala, et al., Phys. Rev. C **91**, 054313 (2015).
 - [32] P. Moller, J. R. Nix, W. D. Myers, and W. J. Swiatecki, Atom. Data Nucl. Data Tabl. **59**, 185 (1995), nucl-th/9308022.
 - [33] A. Lepre tre, H. Beil, R. Berg re, P. Carlos, J. Fagot, A. De Mini ac, and A. Veyssiere, Nuclear Physics A **367**, 237 (1981), ISSN 0375-9474.
 - [34] H. W. Bertini, Phys. Rev. **131**, 1801 (1963).
 - [35] H. W. Bertini, Phys. Rev. **188**, 1711 (1969).
 - [36] A. Fasso, A. Ferrari, J. Ranft and P.R. Sala, SLAC-R-773; (2005).
 - [37] F. Ballarini, et al., Jour. of Phys.:Conf. Series **41**, 151 (2006).
 - [38] J. Levinger, Phys. Rev. **84**, 43 (1951).
 - [39] J. Ahrens, H. Borchert, K. H. Czock, H.B. Eppler, H. Grimm, H. Gundrum, M. Kr ning, P. Riehn, G. Sita Ram, A. Zieger and B. Ziegler, Nucl. Phys. A **251**, 479 (1975).
 - [40] A.B. Larionov and M. Strikman, Phys. Rev. C **101**, 014617 (2020).
 - [41] S. Roesler, R. Engel and J. Ranft, arXiv:0012252 (2000).
 - [42] D. Fabris, G. Viesti, E. Fioretto, M. Cinausero, N. Gelli, F. Lucarelli, J. B. Natowitz, G. Nebbia, G. Prete, et al., Phys. Rev. Lett. **73**, 2676 (1994), URL <https://link.aps.org/doi/10.1103/PhysRevLett.73.2676>.
 - [43] A. Veyssiere, H. Beil, R. Bergere, P. Carlos, A. Lepre tre, Nucl. Phys. A **159**, 561 (1970).
 - [44] P. Carlos, H. Beil, R. Berg re, J. Fagot, A. Lepre tre, A. De mini ac, A. Veyssiere, Nucl. Phys. A **431**, 573 (1984).
 - [45] T. A. Armstrong, W. R. Hogg, G. M. Lewis, A. W. Robertson, G. R. Brookes, A. S. Clough, J. H. Freeland, W. Galbraith, A. F. King, W. R. Rawlinson, N. R. S. Tait, J. C. Thompson, D. W. L. Tolfree, Phys. Rev. D **5**, 1640 (1972).
 - [46] S. Michalowski, D. Andrews, J. Eickmeyer, T. Gentile, N. Mistry, R. Talman, K. Ueno, Phys. Rev. Lett. **39**, 737 (1977).
 - [47] G. Baur, K. Hencken, A. Aste, D. Trautmann, and S. R. Klein, Nuclear Physics A **729**, 787 (2003), ISSN 0375-9474, URL <https://www.sciencedirect.com/science/article/pii/S0375947403001114>.
 - [48] U. Dmitrieva and I. Pshenichnov, Nuclear Instruments and Methods in Physics Research Section A: Accelerators, Spectrometers, Detectors and Associated Equipment **739**, 1114 (2018), ISSN 0168-9002.